Strigolactones And Auxin Cooperate To Regulate Maize Root Development and Response to Nitrate

Cover page

Title

Strigolactones And Auxin Cooperate To Regulate Maize Root Development and Response to Nitrate

Running title

Nitrate-Hormones Crosstalk In Maize Lateral Roots

Corresponding author: S. Quaggiotti; Department of Agronomy, Food, Natural Resources, Animal and Environment

DAFNAE, University of Padova, Viale dell'Università 16, 35020 Legnaro, Padova, Italy.

Telephone number: +39 049 8272913

E-mail: silvia.quaggiotti@unipd.it

Subject areas: (1) growth and development, (2) environmental and stress responses

Tables: 1

Figures: 3 BW, 4 colour

Supplementary Data: 6 datasets, 6 Tables, 3 Figures

This is a pre-copyedited, author-produced version of an article accepted for publication in PLANT & CELL PHYSIOLOGY following peer review. The version of record has been published in Volume 62, Issue 4, April 2021, Pages 610–623, and is available at DOI https://doi.org/10.1093/pcp/pcab014.

Title page

Title

Strigolactones And Auxin Cooperate To Regulate Maize Root Development and Response to Nitrate

Running title

Nitrate-Hormones Crosstalk In Maize Lateral Roots

Authors

Laura Ravazzolo[1], Stéphanie Boutet-Mercey[2], François Perreau[2], Cristian Forestan[3], Serena Varotto[1], Benedetto Ruperti[1], Silvia Quaggiotti[1*]

[1] Dept. of Agronomy, Food, Natural resources, Animals and Environment, University of Padova, viale dell'università 16, 35020 Legnaro, Italy

[2] Institut Jean-Pierre Bourgin, INRAE, AgroParisTech, Université Paris-Saclay, 78000, Versailles, France

[3] Department of Agricultural and Food Sciences (DISTAL), University of Bologna, viale Fanin 44, 40127 Bologna, Italy

***Corresponding author**

Silvia Quaggiotti: Department of Agronomy, Food, Natural Resources, Animal and Environment

DAFNAE, University of Padova, Viale dell'Università 16, 35020 Legnaro, Padova, Italy.

Telephone number: +39 049 8272913

E-mail: silvia.quaggiotti@unipd.it

Abstract

In maize, nitrate regulates root development thanks to the coordinated action of many players. In this study, the involvement of SLs and auxin as putative components of the nitrate regulation of lateral root was investigated. To this aim, the endogenous SL content of maize root in response to nitrate was assessed by LC-MS/MS and measurements of lateral root density in the presence of analogues or inhibitors of auxin and strigolactones were performed. Furthermore, an untargeted RNA-seq based approach was used to better characterize the participation of auxin and strigolactones to the transcriptional signature of maize root response to nitrate.

Our results suggested that N deprivation induces zealactone and carlactonoic acid biosynthesis in root, to a higher extent if compared to P-deprived roots. Moreover, data on lateral root density led to hypothesise that the induction of LR development early occurring upon nitrate supply involves the inhibition of SL biosynthesis, but that the downstream target of SL shutdown, beside auxin, includes also additional unknown players. Furthermore, RNA-seq results provided a set of putative markers for the auxin- or SL-dependent action of nitrate, meanwhile allowing to identify also novel components of the molecular regulation of maize root response to nitrate. Globally the existence of at least four different pathways was hypothesised, one dependent on auxin, a second one mediated by SLs, a third deriving from the SL-auxin interplay and one last attributable to nitrate itself through further downstream signals. Further work will be necessary to better assess the reliability of the model proposed.

Key words

Auxin, Maize, Nitrate, Gene Expression, Lateral Root, Strigolactones

Introduction

Nitrogen (N) is a major nutrient for crops (Kant, 2018; Wang et al. 2018a) and nitrate represents the major N source in aerobic environments (Miller and Cramer, 2004; Gojon, 2017). It acts as a powerful signal modulating the adaptation of root architecture to nitrogen fluctuations in soil (Bouguyon et al. 2012; Undurraga et al. 2017). The knowledge of the mechanisms underlying the nitrate signalling pathway is of crucial importance to improve Nitrogen Use Efficiency (NUE) of crops and to limit the environmental impact of the excessive distribution of fertilizers (Hirel and Lea, 2018; Kant et al. 2011; Li et al. 2017).

In cereals the root system includes primary root (PR), lateral roots (LR), and a shoot-borne system of crown and seminal roots (CR and SR, respectively) (Smith and De Smet, 2012). Generally, LR are more sensitive to nitrate levels than PR (Tian et al. 2014), but this process is rather complicated (Sun et al. 2017 and references therein) and dependent on both the genotype and the environment (Yu et al. 2015a; Xuan et al. 2017). Up to now few lateral root mutants have been described in monocots and they are generally auxin-related (Hochholdinger and Tuberosa, 2009; Atkinson et al. 2014; Yu et al. 2018; Yu et al. 2019; Du and Scheres, 2018). However, differently from Arabidopsis for which the participation of auxin to the signalling governing the nitrate regulation of lateral root development has been widely recognised (Vidal et al. 2013; Mounier et al. 2014; Xu and Cai, 2019; Zhang et al. 2019), only limited information is available for cereals.

In maize, N-deprivation induces the exudation of strigolactones (SLs) by roots and inhibits lateral root development and both these processes are readily reversed in response to nitrate provision (Trevisan et al. 2015; Manoli et al. 2016, Ravazzolo et al. 2019). Furthermore, Ravazzolo et al. (2019) also hypothesised that the stimulation of maize lateral root development observed in response to nitrate could in part depend on the shutdown of strigolactone (SLs) production.

The negative regulation of LR development by SLs has been already documented in Arabidopsis and rice, which developed a lower number of lateral root primordia (LRP) when plants were treated with a SL analogue (*rac*-GR24), namely the racemic mixture of the two enantiomers $GR24^{5DS}$ and $GR24^{ent\text{-}5DS}$ (Ruyter-Spira et al. 2011; Sun et al. 2014, 2019a; Marzec and Melzer, 2018).

In light of the role played by SLs on shoot and root branching, a number of studies on rice (Arite et al. 2007) and Arabidopsis (Bainbridge et al. 2005) focused on their interactions with auxin, that seems to induce SL biosynthesis genes both in shoots and roots (Rameau et al. 2019). In addition, in pea it was proposed that SLs may regulate auxin biosynthesis in the shoot through a direct repressive effect on the expression of auxin biosynthesis genes (Ligerot et al. 2017).

On the other hand, in Arabidopsis SLs negatively regulate the PIN auxin efflux carriers family, thus interfering with the polar auxin transport (PAT) and auxin canalization both in the shoot and in the root (Koltai et al. 2010; Shinohara et al. 2013; Ruyter-Spira et al. 2011). Accordingly, SL-biosynthesis mutants show higher PINs levels and increased auxin transport (Liang et al. 2016).

In maize, a reallocation of PINs by cytoskeleton remodelling was hypothesised to occur already after two hours of nitrate provision to N-deprived root (Manoli et al. 2016), thus reinforcing the idea that nitrate-induced root architectural adjustments could depend on auxin re-distribution and leading to hypothesise an interplay between strigolactones and auxin. In maize basipetal auxin transport is facilitated by PIN auxin efflux carriers in response to local nitrate supply (Yu et al. 2016). For instance, the monocot-specific *ZmPIN9* gene expressed in phloem pole cells modulates auxin efflux to pericycle cells leading to subsequent cell cycle activation (Yu et al. 2019).

PINs and a number of additional target genes (Jansen et al. 2013; Tai et al. 2016) would represent putative candidates to assess the auxinic involvement in the lateral root development in response to nitrate and also to address the hypothetical involvement of strigolactones in the overall process.

The present work is aimed at deepening our knowledge on synergistic or independent actions of auxin and strigolactones in the achievement of the nitrate regulation of lateral root development, through a multiple approach based on chemical, physiological and molecular analyses. The amount of SLs (namely zealactone and carlactonoic acid) in root tissues was determined by LC-MS/MS and the lateral root density was measured in N-deprivation, upon nitrate supply and in the presence of both synthetic auxin and SLs and their inhibitors. Furthermore, a systemic molecular study based on RNA-sequencing was adopted, enabling the definition of four subgroups of genes, whose transcription was regulated in maize root in response to nitrate and in dependence of auxin, SLs, both of them or of further downstream players. This approach led to identify a number of molecular targets which distinguish each signalling pathway as well as shared elements, which may represent crucial factors in the process leading to maize root adaptation to N fluctuations.

Results

N-starvation and nitrate differently affect SL biosynthesis in plant tissues

The strigolactones were detected, annotated, and quantified as described in Ravazzolo et al. (2019) in root tissue of seedlings exposed to 24h of nitrate-supply ($+NO_3^-$) or N-starvation (-N) after a 24h-pre-incubation under N-deficient conditions or to phosphate-starvation (-P). As zealactone was unavailable either in isotope-labelled form or in unlabelled form, the commercially available synthetic strigolactone GR24 was used as an internal standard in order to obtain a relative quantification of zealactone. This internal standard could then

compensate matrix effects that were non-specific or strigolactones-specific. The strigolactone found at 10.8 min has been annotated as the same zealactone isomer as in Ravazzolo et al. (2019). Similarly, a second compound was detected at MRM channels *m/z* 333>97 and 333>219 at 11.3 min, both transitions corresponding to published transitions for protonated carlactonoic acid (Charnikhova et al. 2017) and to no other known strigolactone. One supplementary MRM transition *m/z* 355>258 was observed at the same retention time (**Supplementary Table S1**). This could correspond to a strigolactone sodium adduct ion (M+23) losing its D cycle. All these elements suggested that this suspected strigolactone had a molecular weight of 332 and was a putative carlactonoic acid. Accordingly, carlactonoic acid was produced in response to N-starvation in a qualitatively similar manner compared to zealactone (0.48 ng eq GR24/g root tissue), and even more intensely, as it was also well induced in response to phosphate-deprivation (0.22 ng equivalent GR24 per g root tissue), which was utilized as a positive control for SL production (Umehara et al. 2010; Kumar et al. 2015), while it was not detected at all in response to nitrate provision. The putative zealactone isomer was detected at a significant level (0.12 ng equivalent GR24 per g root tissue) in samples obtained from phosphate-starved seedlings. Not surprisingly, this compound was detected at a much higher level (0.45 ng eq GR24/g root tissue, P=0.11) in nitrogen-starved samples. In contrast, nitrate-supplied samples contained very low zealactone isomer (0.11 ng eq GR24/g root tissue, P=0.11), suggesting an inhibitory effect of nitrate on zealactone production (**Fig. 1A**). Therefore, high levels of carlactonoic acid could be regarded as a signature of N-deprivation, similarly or even better than zealactone, provided that the difference between carlactonoic acid levels in -P and -N are significantly different (**Fig. 1B**). Nevertheless, the production of both appeared to be strongly impeded in nitrate-supplied plants.

.

Nitrate regulation of LR development depends on auxin and SLs

As previously shown (Ravazzolo et al. 2019), nitrate significantly induced LR formation ($+NO_3^-$) in comparison to roots of maize seedlings grown in a N-deprived medium (-N) (**Fig. 2**). To investigate the mechanisms for this regulation, several single or combined treatments with auxin (NAA), an inhibitor of auxin action (PCIB), strigolactone (GR24) and an inhibitor of strigolactone biosynthesis (TIS108) were performed (**Fig. 2**). Since the cell cycle time in maize LRP cells has been estimated to be approximately 4.5 h (Macleod and Thompson, 1979), and it was estimated that it takes 14 h for pericycle cells located at the upper limit of the meristem to reach the level of LR initiation (Alarcón and Salguero, 2017), a time lapse interval of 24 h was chosen to compare the effects of the different treatments tested, thus enabling the detection of LRP, starting from 20 mm from the root tip as small brown dots to larger and more defined dots in the more differentiated zone under the seed.

The provision of PCIB to nitrate-supplied plants significantly reduced the density of LR, even though not to the levels observed for N-deprived roots (CTR-).

To assess if exogenous auxin provided to N-deprived plants was able to re-establish the phenotype observed for nitrate-supplied plants ($+NO_3^-$) four increasing concentrations of NAA (a, 0.01 µM; b, 0.05 µM; c, 0.1 µM; and d, 1 µM) were tested. All the four treatments (**Supplementary Figure S1**) triggered a significant increase of LR number, but in all cases with values significantly lower than those observed for nitrate-treated seedlings ($+ NO_3^-$). For most of the subsequent experiments the lowest NAA concentration (0.01 µM) was utilised since higher concentrations did not result in further enhancement of LR induction. The delivery of PCIB to NAA-provided plants strongly inhibited the development of LR, however in this case the degree of the inhibition was much more noticeable than that observed when PCIB was provided to nitrate supplied plants. These results suggest that the effects of nitrate on LR development are dependent on auxin, but that also auxin-independent components might take part in the overall process.

As expected (Ravazzolo et al. 2019), the provision of GR24 to nitrate supplied plants strongly inhibited the development of LR, further confirming the hypothetical role of SLs as negative regulators of LR development. When NAA (0.01 µM; 0.05 µM; 0.1 µM;) was supplied together with GR24 (**Fig.2**; **Supplementary figure S1**) the production of LR was re-established, even though to a lesser extent in comparison to the effect triggered by nitrate.

Accordingly, the provision of TIS108 to N-deprived seedlings restored the $+NO_3^-$ phenotype, leading to an even higher number of LR, possibly due to the complete inhibition of SL biosynthesis, that upon nitrate provision could be still slightly present. To verify if this action depended on a restoration of the auxinic activity TIS108 provided plants were also treated with PCIB (**Fig. 2**). This treatment led to a significant reduction of LR density, but the LR number was still considerably higher than that observed in –N. Globally these results support the idea that the inhibition of SL could reactivate auxin signalling/action and that this mechanism could at least in part be responsible for the stimulation of LR development by nitrate. However, they also suggest that further components beside auxin would be involved in the nitrate signalling and in the SL-dependent regulation of LR in response to nitrate.

Auxin regulation of* CCD8 *and* WBC33 *and inhibition of* Phelipanche ramosa *germination

Basing on above results the inhibition of SL biosynthesis observed upon nitrate supply might induce auxin action. To investigate if auxin negatively affects SL production the expression of *CCD8*, a reliable marker for SL biosynthesis in maize (Ravazzolo et al. 2019; Guan et al. 2012), was analysed. As expected, its transcription was strongly down-regulated when nitrate was provided to -N-plants, however no significant changes were noticed in response to NAA provision, leading to hypothesise that the inhibition of its

transcription by nitrate might be independent from auxin (**Fig. 3A**). On the contrary, the transcription of *WBC33*, that has been hypothesised to participate to SL transport (Ravazzolo et al. 2019), was noticeably down-regulated both by nitrate (as expected) and by auxin (**Fig. 3B**), suggesting that auxin might affect the SL transport mainly through *WBC33,* putatively involved in the exudation of SLs. However, the accumulation of transcripts for both of these genes was not significantly altered in response to PCIB.

To further deepen this hypothesis, the presence of SLs in the exudates was indirectly assessed through a bioassay based on *Phelipanche ramosa* germination. Exudates derived from N-deprived plants strongly induced *P. ramosa* germination, and both nitrate and auxin significantly reduced it (**Fig. 3C**), even though nitrate is more effective than auxin (12 times lower germination rate in nitrate-supplied plants, 2.5 times lower germination rate with NAA provision with respect to N-deficient medium, respectively). These findings support the hypothesis that the auxinic component of nitrate signalling is involved in inhibiting SL transport outside the root and further support the already hypothesised role of WBC33 as an exporter of SLs (Ravazzolo et al. 2019).

Nitrate regulation of maize root transcriptome depends on cross-talks between auxin, SLs and on further signalling pathways

To better assess the crosstalk existing among nitrate, auxin and SLs in the regulation of maize root response to nitrate an untargeted transcriptomic approach was utilized. RNA-Seq Illumina sequencing of RNA samples obtained from -N, $+NO_3^-$, -N +TIS108 and $+NO_3^-$ +PCIB treated plants resulted in 23 to 33 million high-quality reads per biological replicate (**Supplementary Table S2**), with about 97% of them mapped on the maize B73 reference genome. DESeq2 R-package was then used for differential expression analysis after estimation of gene transcript abundances in the different conditions (**Supplementary dataset 1-2-3-4-5-6**). The genes showing a log2 fold change ratio >|1| (corresponding to a 2-fold change variation in expression level) and a false discovery rate (FDR) adjusted *p* value ≤ 0.05 in the $+NO_3^-$/-N comparison were considered as differentially expressed genes (DEGs), resulting in 1333 DEGs significantly responsive to NO_3^-. Among them, the great majority were down-regulated by nitrate provision (90%), while only 10% were up-regulated (**Fig. 4A**). To identify genes significantly responsive to nitrate but also responsive or unresponsive to TIS108 and/or PCIB, the log2 fold change threshold was decreased to 0.58 (corresponding to a 1.5-fold change variation in expression level) for the remaining comparisons, leading to identify 998 DEGs in the comparison between -N+TIS108 and -N; 430 between -N+TIS108 and $+NO_3^-$, 1313 between $+NO_3^-$ +PCIB and -N and 1575 between $+NO_3^-$ +PCIB and$+NO_3^-$. Integration of DEGs identified in the different pairwise comparison allowed to identify 848 DEGs significantly responsive to both nitrate and at least one of the other treatments (-N +TIS108; $+NO_3^-$+PCIB), as shown in **Fig. 4B**.

Clusters of gene expression according to TIS108- and PCIB-responsiveness

Hierarchical clustering of the 848 DEGs significantly responsive to nitrate and to PCIB and/or TIS108 was performed. This allowed to manually dissect four different clusters based on the TIS108-responsiveness and the PCIB-responsiveness (**Supplementary Figure S2; Supplementary Table S3**). Accordingly, Cluster 1 grouped together 294 DEGs TIS108-responsive and PCIB-unresponsive, Cluster 2 grouped together 101 DEGs unresponsive to both TIS108 and PCIB, Cluster 3 grouped together 425 DEGs responsive to both TIS108 and PCIB, while Cluster 4 grouped together 28 DEGs TIS108-unresponsive and PCIB-responsive.

A further inspection of genes belonging to clusters 1, 3 and 4 led to sub-select only the genes whose regulation by nitrate seems to involve SL repression (263 out of 294 DEGs in Cluster 1), SL repression and auxin induction (269 out of 425 DEGs in Cluster 3) or only auxin induction (all the 28 DEGs in Cluster 4) respectively, while for cluster 2, which include DEGs unresponsive to TIS108 and PCIB, no further selection was necessary (101 DEGs) (**Fig. 5A**). In particular, among cluster 1 were selected only those DEGs with a similar expression trend among $+NO_3^-$ and -N +TIS108 treatments (subgroup of Cluster 1). In cluster 3, DEGs were selected for their similar expression values among $+NO_3^-$ and -N +TIS108 treatments, and opposite trend among $+NO_3^-$ and $+NO_3^-$ +PCIB treatments, thus displaying a putative SL- and auxin-dependency related to nitrate provision (subgroup of Cluster 3). In cluster 4, all 28 DEGs showed a gene expression trend opposite among $+NO_3^-$ and $+NO_3^-$ +PCIB treatments, so they were maintained for their putative auxin-dependency related to nitrate provision.

A KEGG mapper pathways reconstruction was then used to show pathways displaying significant changes based on DEGs of the four groups (**Fig. 5B**; **Supplementary Table S4**). DEGs were assigned to 45 pathways for subgroup of Cluster 1, 30 pathways for Cluster 2, 72 pathways for subgroup of Cluster 3 and 8 pathways for Cluster 4. All clusters were characterized by the identification of common pathways (e.g., the phenylpropanoid biosynthesis to obtain lignin or the plant hormone signal transduction), but clusters 1, 2 and 3 also displayed unique components. Contrarywise, in the case of transcripts belonging to Cluster 4, no specific signatures were noticed.

In particular, pathways related to brassinosteroids biosynthesis and jasmonate signalling were a typical feature of transcripts whose regulation by nitrate involve the SL inhibition (subgroup of Cluster 1), pathways related to sulphur metabolism, cytokinin signalling and vesicular transport were instead a trait of transcripts regulated by nitrate independently of both SLs and auxin (Cluster 2) and those related to cell membrane and cell wall, RAP1, MAPK and calcium signalling were predominantly represented among transcripts regulated by nitrate in a SLs/auxin dependent manner (subgroup of Cluster 3).

Nitrate affects the expression of specific auxin marker genes

Six genes encoding key players of auxin signalling and transport and being differentially regulated in response to nitrate (**Supplementary Table S6**) were selected for further expression analyses. *IAA24* belongs to subgroup of cluster 1, *ARF4* and *TAZ2* belong to cluster 2, *PIN9* and *HSP101* belong to the subgroup of cluster 3, and *ARF20* belongs to cluster 4 (**Fig. 6, Supplementary Table S5**).

IAA24 transcripts decreased in response to nitrate but did not significantly change in the presence of exogenous auxin, neither when PCIB was provided together with nitrate. Nevertheless, TIS108 (provided to N-deprived plants) down-regulated its expression and GR24 (provided to nitrate-supplied plants) slightly re-induced its transcription, thus confirming its belonging to the cluster 1, which collects transcripts regulated by nitrate likely through SL inhibition but not through auxin induction.

ARF4 and *TAZ2* both belonging to cluster 2 (unresponsive to TIS108 and PCIB) were both up-regulated by nitrate, but while *ARF4* showed up-regulation also in response to NAA, the transcription of *TAZ2* was not significantly affected. The transcription of *ARF4* induced by the provision of NAA to nitrogen-depleted plants is in partial contrast with its belonging to cluster 2. However, PCIB induced no significant variation nor on *ARF4* or on *TAZ2* expression, thus confirming their PCIB-unresponsive behaviour evidenced by RNA-seq. Furthermore, the expression of both *ARF4* and *TAZ2* was not significantly altered by nor TIS108 or GR24, as expected according to RNA-seq data.

PIN9 (cluster 3, responsiveness to both SLs and auxin) transcription was clearly induced by nitrate and inhibited when PCIB was provided to the nutritional medium, thus indicating also in this case an auxinic activity of nitrate. However, despite this, no effects were observed in the presence of exogenous NAA. TIS108 provided to N-deprived roots induced *PIN9* transcription confirming the expression noticed in RNA-seq analyses, allowing to confirm its SL-dependency, even if the provision of GR24 to nitrate-supplied plants did not inhibit its expression.

HSP101 (cluster 3, responsiveness to both SLs and auxin) was down-regulated by nitrate provision, and up-regulated by PCIB. Furthermore, even though the provision of NAA to N-deprived roots did not induce a similar down regulation of their transcription, PCIB together with NAA strongly up-regulated it, resembling the trend observed when PCIB was provided to nitrate supplied plants, leading to confirm the supposed involvement of this transcript in the auxin-dependent nitrate gene regulation. Besides, *HSP101* transcription was reduced in response to TIS108 provision to -N plants, thus confirming the involvement of SLs in this mechanism, but not restored by the supply of GR24 to nitrate-fed plants.

Finally, the transcription of *ARF20* (cluster 4, auxin dependent) was up-regulated by nitrate, but also by NAA, while PCIB reversed this trend in both cases. However, its expression was not significantly altered by TIS108 and GR24 treatments, confirming its attribution to cluster 4.

To sum up, nitrate regulation of *ARF20* transcription seems to be auxin-dependent, *IAA24* regulation seems instead depend more on SL inhibition observed upon nitrate provision, *HSP101* and *PIN9* are proposed to respond to nitrate through a complex mechanisms in which SL inhibition and auxin induction are connected, and finally *ARF4* and *TAZ2* would seem to be exclusively responsive to nitrate (**Fig. 7**).

Discussion

Nitrate regulates root development (Zhang and Forde, 2000; Sun et al. 2017; Undurraga et al. 2017) and this is crucial to accomplish adaptation to N fluctuations and to achieve NUE (Kant, 2018; Plett et al. 2018). Hence, the comprehension of the mechanisms underlying this plasticity could provide crucial information to select plants better adapted to low N and more plastic to its variations (Iqbal et al. 2020).

In this paper we displayed new evidence that N-deficiency could strongly induce SL biosynthesis in maize roots (**Fig. 1**), consistently with our previous hypothesis (Ravazzolo et al. 2019). Zealactone was already demonstrated to represent the most important maize SL upon N-starvation, but the present results indicate that also carlactonoic acid (CLA) could mark this condition in roots. Carlactonoic acid is obtained by oxidization from carlactone (CL) and it is the putative intermediate of both the strigol-type and orobanchol-type SLs (Matusova et al. 2005; Abe et al. 2014). In addition, CLA is also the precursor of the non-canonical SL called zealactone (Charnikhova et al. 2017). Based on these results it is possible to hypothesise two alternative scenarios, one in which both these SLs could function to signal and regulate N-deprivation response and a second one in which CLA would be only an intermediate in the biosynthesis of zealactone, that would represent the unique SL marking the N-starvation condition. The detection of carlactonoic acid only in roots and not in exudates (Ravazzolo et al. 2019) could lead us to speculate a third scenario, where N-deprivation starts a two-tier signalization pathways, one within the plant (carlactonoic acid), the other outside the plant (zealactone) to regulate neighbour roots or relationship with the rhizosphere.

The mechanisms through which nitrate regulates LR development is complex and only partially known, especially in monocots (Sun et al. 2017; Forde, 2014; Yu et al. 2015a; Xuan et al. 2017). LR are crucial organs to explore soil and uptake water and nutrients, and they are more sensitive to variations in nitrogen than PR (Tian et al. 2014; Hachiya and Sakakibara, 2017). Results observed with synthetic auxin (NAA) or auxin inhibitor (PCIB) treatments suggest that the nitrate regulation of LR development could in part depend on

auxinic activity, even though further components seem to be also involved, leading to hypothesise the existence of both auxin-dependent and auxin-independent effects of nitrate (**Fig. 2**). In addition, synthetic SL (GR24) strongly inhibits the nitrate induction of LR development, and the SL biosynthesis inhibitor TIS108 provided to N-deprived plants re-established the typical nitrate LR phenotype, as previously showed by Ravazzolo et al. (2019). The negative regulation of LR development by SLs is acknowledged also in Arabidopsis and rice (Ruyter-Spira et al. 2011; Sun et al. 2014).

If the SL phenotype depends on the suppression of auxin biosynthesis presumably occurring in -N roots, NAA provision to plants treated with nitrate and GR24 would re-induce the proliferation of LR to levels similar to those observed in the presence of nitrate alone. However, in our conditions the nitrate phenotype was only partially restored. These data globally suggest that the induction of LR development early occurring upon nitrate supply involves the inhibition of SL biosynthesis, while the downstream targets of SL shutdown, beside auxin sensitivity/signalling, may include also additional unknown players. A model based on the interaction of SLs and auxin to regulate root development has been proposed also by Ruyter-Spira et al. (2011) and by Koren et al. (2013).

The repression of the expression of genes involved in auxin biosynthesis by SLs was already hypothesised in pea by Ligerot et al. (2017). Furthermore, Hayward et al. (2009) and Prusinkiewicz et al. (2009) demonstrated that auxin affects SL metabolism and signalling by regulating gene expression. The present results showed that the provision of exogenous NAA to N-depleted plants, while stimulating LR development, did not affect the transcription of *CCD8*, which represents a marker for SL biosynthesis in maize (Ravazzolo et al. 2019), but it noticeably downregulated both the transcription of *WBC33* (encoding a putative SL transporter) and the exudation of SLs by roots (**Fig. 3**).

To better characterize the molecular components of this complex scenario, thanks to a systemic approach based on RNA-sequencing (**Fig. 4**), nitrate regulated genes were assigned to 4 sub-groups according to their dependency on PCIB or TIS108 or on both of them (**Fig. 5A**), enabling to highlight specific and common molecular signatures characterizing the different mechanisms of action of nitrate (**Fig. 5B**). The auxin signalling pathway was shared among the four clusters, strengthening the hypothesis that nitrate regulation of root response strongly depends on its regulation, while many other terms were specifically attributed to each cluster, as shown in **Fig. 5B**. Further hormonal signalling was demonstrated to belong specifically to an individual subgroup of transcripts. Furthermore, novel molecular targets of nitrate were identified as putative regulators of the maize root response to this nutrient in an auxin, SLs, auxin/SLs dependent or independent manner.

Six genes related to auxin and/or LR development were selected and their expression was studied more deeply by qPCR (**Fig. 6**). *IAA24*, *TAZ2* and *ARF20* displayed a transcriptional response to NAA or GR24 always consistent with what was expected from the clustering results, while *ARF4*, *PIN9* and *HSP101* transcription was partially incoherent. The incongruence emerging when comparing gene expression in response to PCIB and NAA might be the consequence of the action of PCIB as auxin antagonist. In fact, since it impairs auxin signalling through the regulation of Aux/IAA stability (Oono et al. 2003), targets operating upstream of Aux/IAA degradation or involved in auxin transport could not be affected by PCIB provision. Besides, this discrepancy might also depend on the fact that exogenous NAA does not mimic eventual effects of nitrate which could affect endogenous auxin in a cell specific manner. Regarding GR24-unresponsiveness, despite the canonical SL GR24 is still the most widely used synthetic SL for bioassay (Zwanenburg et al. 2016), it might induce unexpected *in vivo* responses in maize, due to the existence of non-canonical SLs (Charnikhova et al. 2017).

According to present results, nitrate regulation of *IAA24* transcription seems to uniquely depend on SLs. In Arabidopsis, the homolog of maize *IAA24* is *IAA3/SHORT HYPOCOTYL2 (SHY2)*, a negative regulator of the root meristem development (Li et al. 2020) that is repressed during the SL regulation of meristem size and LR formation (Koren et al. 2013), in accordance with our results.

Auxin/INDOLE-3-ACETIC ACID (Aux/IAA) proteins interact with ARFs (Auxin Response Factors) preventing their binding to DNA thus controlling the expression of genes encoding transcription factors involved in the downstream auxin response in root development (Ludwig et al. 2013, Du and Scheres, 2018, Alarcón et al. 2019). The transcription of *ARF20* was up-regulated in response to both nitrate and auxin, leading to the hypothesis that it could play key roles in the auxin-mediated regulation of root development by nitrate. In addition, *ARF4* transcription was induced in response to nitrate and auxin, even if it resulted PCIB-unresponsive, representing a case of partial incongruence among clustering and qPCR results, as stated above.

Maize *TAZ2* encodes a BTB/POZ and TAZ domain-containing protein 2 (BT2 protein) whose expression in Arabidopsis is regulated by a number of signals including nitrogen (Mandadi et al. 2009) and seems to be part of a feedback loop that enhances specific responses to exogenous auxin (Ren et al. 2007; Robert et al. 2009). Present results indicate that the regulation of *TAZ2* expression in maize roots in response to nitrate responds directly to this nutrient itself, likely in an auxin/SLs independent way. On the contrary, *HSP101* which encodes a heat shock protein of 101 kDa induced by heat and drought (Nieto-Sotelo et al. 2002) and involved in the auxin-mediated maize crown root development (Martínez-de la Cruz et al. 2015), seems to participate to the nitrate regulation of maize in an auxin and SLs-dependent manner.

The induction of the transcription of the monocot-specific *ZmPIN9* by nitrate seems to depend on auxin and SLs, even though, as stated above, treatment with NAA and GR24 led to a transcription profile incoherent with the hypothesis derived by RNA-seq results. Auxin canalisation in lateral root primordia is regulated at all stages of LR development by different

members of the PIN family (Benková et al. 2003). It has been already suggested that SLs interfere with polar auxin transport (PAT) and auxin canalization both in the shoot and the root in Arabidopsis (Shinohara et al. 2013, Ruyter-Spira et al. 2011) mainly by the negative regulation of both the transcription of *PINs* genes and their relative polar localization at the plasma membrane (Soundappan et al. 2015; Liang et al. 2016). Accordingly, SL-biosynthesis mutants show higher PINs levels and increased auxin transport (Liang et al. 2016). Globally these data allowed to gain new knowledge on the mechanisms underlying the regulation of LR development by nitrate and more in general the maize root response to this anion. At least four independent mechanisms are supposed to exist (A, B, C and D), each of which featured by specific transcriptional signatures (**Fig. 7**), as emerged from the clustering analysis of the RNA-seq data (**Fig. 5**) and then confirmed by targeted expression analyses (**Fig. 6**). Four additional genes were included in our model, based on their putative functions in auxin signalling or LR formation: *IAA5*, *YUCCA6*, *ARGOS7* and *SOMBRERO* (**Fig. 7**). *IAA5* is a NAA-inducible Aux/IAA transcription factor highly expressed in lateral root if compared to primary or seminal roots (Ludwig et al. 2013). *YUCCA6* encodes an indole-3-pyruvate monooxygenase involved in auxin synthesis from tryptophan (Nishimura et al. 2009). *ARGOS7* (Auxin-Regulated Gene Involved in Organ Size 7) is involved in lateral organ size in Arabidopsis through the AXR1 (Auxin Resistant 1)-dependent auxin signalling pathway (Hu et al. 2003; Shi et al. 2016). Finally, *SOMBRERO* (*SMB*) encodes a NAC domain transcription factor that in Arabidopsis is expressed in in the outermost layer of the LR primordium tip (LRPs, stage VI) (Du and Scheres, 2017), accordingly to its presumed role in specifying root cap progenitor cells (Willemsen et al. 2008). Bases on these data a crosstalk between different pathways should be hypothesised (**Fig. 7**): a first scenario implies that nitrate exerts its action by inducing the auxinic response in roots (A), a second hypothesis assumes that it acts by lowering the biosynthesis of SLs independently of auxin (B), while a third scenario leads to suppose a coordinated interplay between auxin and SLs in which the auxin induction seems to depend on the inhibition of SL production (C). Finally, a scenario in which nitrate regulates this process independently of both auxin induction and SL inhibition (D) should be also acknowledged.

Besides representing useful markers for the different signalling pathways above described, the set of transcripts here identified also provide new knowledge on the molecular regulation of maize root response to nitrate, leading the way to novel hypotheses to be deepened hereafter.

Lastly, our preliminary data also suggest that auxin itself could inhibit the exudation of SLs possibly by down-regulating the expression of a putative SL transporter (*ZmWBC33*).

Further and more detailed SLs and auxin content measurements in the presence of their inhibitors and analogues should be performed to make the model more reliable. The employment of maize mutants for genes listed in **Fig. 7** will be useful to gain functional confirmation of our model. For now, *hsp101* would seem the most suitable candidate, since mutants for this gene, obtained using a reverse genetics approach, are already available and were used to study thermotolerance and primary root growth (Nieto-Sotelo et al. 2002). Nevertheless, despite the need of further functional validation, our findings provide new knowledge on the process leading to the overall maize root response to N fluctuations.

Materials and Methods

Maize growth conditions

Seeds of the maize inbred line B73 (*Zea mays* L.) were germinated as described by Manoli et al. (2014). After germination, seedlings were grown for 24h in a N-deprived solution (-N) and then transferred to 14 different treatments, as reported in **Table 1.**

6-phenoxy-1-phenyl-2-(1H-1,2,4-triazol-1-yl) hexan-1-one (TIS108) and $GR24^{5DS}$ (Strigolab, Torino, Italy) were used as inhibitor of SL biosynthesis (Ito et al. 2011) and synthetic SL analogue, respectively. p-chlorophenoxyisobutyric acid (PCIB) and 1-naphthaleneacetic acid (NAA) were used as auxin signalling inhibitor (Oono et al. 2003) and synthetic auxin analogue, respectively. NAA was used as a further control to compare the effects observed upon nitrate provision with those resulting from NAA supply. Unless stated otherwise, all chemicals were obtained from Sigma Chemicals (Sigma, St Louis, MO, USA).

For the SL quantification on root tissue, basing on the known SL induction by P starvation, an additional positive control with P-deprived plants was included.

A growth chamber with a day/night cycle of 14/10 h at 25/18°C air temperature, 70/90% relative humidity, and 280 μmol $m^{-2} \cdot s^{-1}$ photon flux density was used.

SL identification and quantification in root tissue

All root system was sampled from 10 seedlings for every treatment (nitrate-supplied, $+NO_3^-$; N-deficient, -N, phosphate-starved, -P), in three independent biological repetitions, and immediately frozen and powdered in liquid nitrogen. According to our previous study (Ravazzolo et al. 2019), the result from phosphate-starved seedlings was utilized as a positive control for SL exudation. The powder was extracted twice with 3 mL ethyl acetate (EtOAc) containing 10 ng of GR24 as an internal standard, the supernatants were pooled and dried before to be purified through the silica solid phase extraction as described by Boutet-Mercey et al. (2018). All the different fractions were quantified by LC-MS/MS analysis, MRM mode, as described by Ravazzolo et al. (2019). Data are reported as mean ± SE of three replicates.

Lateral root analysis

The lateral root density was measured using the Image J Image Analysis Software and the LR density was expressed as percentage compared to the value observed for nitrate-provided roots (positive control; treatment ID = 2). Root images were collected using a flatbed scanner. To better visualize LRP a haematoxylin staining solution supplied with ferric ammonium sulphate was used, as described by Ravazzolo et al. (2019). Three biological replicates for each treatment and an ANOVA statistic test were performed (n=30).

RNA extraction and sequencing library preparation

Among the 14 treatments, 4 were used to obtain their transcriptomic profile by means of RNA-sequencing technique: -N (1), $+NO_3^-$ (2), -N +TIS108 (3), $+NO_3^-$ +PCIB (5). After 24 h in the equivalent treatment, each whole root was sampled from 4 pooled seedlings for treatment, in three independent biological repetitions, and immediately frozen in liquid nitrogen. Total RNA was extracted using Spectrum™ Plant Total RNA Kit (Sigma, St Louis, MO, USA). RNA was quantified with a Nanodrop1000 (Thermo Scientific, Nanodrop Products, Wilmington, DE, USA). RNA quality was assessed via agarose gel electrophoresis and a Bioanalyzer (Agilent Technologies, Santa Clara, CA, United States). For all samples, a RIN (RNA integrity number) $\geq$ 8.0 was detected. cDNA libraries for Illumina sequencing were constructed according to the instructions of the manufacturer (TruSeq stranded mRNA Sample Preparation; Illumina, San Diego, CA, United States). Sequencing was performed at the Centro di Ricerca Interdipartimentale per le Biotecnologie Innovative (CRIBI, Padova, Italy), on a NovaSeq 6000 instrument (Illumina).

Processing of Sequenced Reads and Differential Expression Analysis

Base calling was performed using the Illumina Pipeline. Quality of the resulting raw reads (23–33 million of read pairs per library) was initially checked using FastQC 0.11.9 (Andrews, 2010); reads were then processed for adapter clipping and quality trimming using Trimmomatic 0.39 (Bolger et al. 2014). The biological replicate defined as R3 for the $+NO_3^-$ +PCIB treatments presented a high percentage of rRNA-related reads, resulting in low percentage of high-quality reads (29%) with respect to the total number of read pairs (**Supplementary Table S2**). The resulting high-quality reads were mapped to the maize B73 reference genome (RefGen ZmB73 Assembly AGPv4 and Zea_mays.AGPv4.47.gtf transcript annotation retrieved from EnsemblPlants (Jiao et al. 2017) with Tophat 2.0.13 (Kim et al. 2013) using the following modifications from default parameters: maximum intron size, 60,000; minimum intron size, 10; up to three mismatches and gaps allowed. The sequence alignment files (BAM format) were then filtered using Samtools (Li et al. 2009) to remove alignments with MAPQ smaller than 1 (corresponding to multi-mapped reads assigned to more than 10 different genomic positions). Gene-level read counts for each sample were generated using the featureCounts Subread package v 2.0.1 (Liao et al. 2019; Liao et al. 2014), with the –M, -O, --fraction, and --ignoreDup options.

Starting from the produced gene count matrix, the structure and the goodness of the data were revealed by sample distance matrix and PCA using the R (https://www.r-project.org) (v3.6.1) package DESeq2 (v1.30; Love et al. 2014). Counts-based PCA plot clearly indicate that replicate 3 of the $+NO_3^-$ +PCIB treatment did not correlate with the other replicates (R1 and R2) of the same treatment (**Supplementary Figure S3**) and was therefore excluded from further differential expression analysis.

DESeq2 package was used to calculate gene normalized expression values (**Supplementary dataset 1**) and to identify differentially expressed genes (DEGs) among different treatments. Genes showing an FDR-adjusted p-value (padj) < 0.05 and log2 fold change (log2FC) > |0.58| or > |1| were considered as DEGs in the comparisons among the different samples (see Results and **Supplementary datasets 2-3-4-5-6**). RNA-Seq data from this article can be found in the Gene Expression Omnibus data library under accession number GSE162411 (https://www.ncbi.nlm.nih.gov/geo/query/acc.cgi?acc=GSE162411, secure token for reviewer access: enmtciggxfmzzyv).

Functional annotation and gene selection

Venn diagram (https://bioinfogp.cnb.csic.es/tools/venny/) was used to compare and integrate DEGs responsive to nitrate and in at least one of the other treatments. Hierarchical clustering of these selected DEGs was then performed by average linkage and Pearson distance using the Morpheus software (https://software.broadinstitute.org/morpheus/) and displayed as a heat map. This clustering allowed to dissect four different clusters basing on the profile of TIS108 and the PCIB responsiveness. To identify the most important metabolic pathways among the four clusters, DEGs were aligned to KEGG (Kyoto Encyclopedia of Genes and Genomes) database using the KEGG Reconstruction Pathway tool (https://www.genome.jp/kegg/), and the resulting pathways were visually represents using the DiVenn tool (https://divenn.noble.org/; Sun et al. 2019b). Finally, Gene Ontology (http://geneontology.org/) was used to look for genes involved in auxin signalling and transport and root development. Therefore, 6 differentially expressed genes (DEGs) statistically significant with a p-value<0.05 were obtained (**Supplementary Table S6**): *IAA24*, *ARF4*, *ARF20,* and *TAZ2* enriched for the GO term related to auxin-activated signalling pathway (GO:0009734); *PIN9* enriched for the term related to auxin polar transport (GO:0009926), *HSP101* enriched for the term related to the regulation of root development (GO:2000280).

The expression of a SL biosynthesis gene (*CCD8;* Guan et al. 2012) and of a putative SL transporter (*WBC33*; Ravazzolo et al. 2019) was also measured in response to auxin treatments (Ravazzolo et al. 2019).

cDNA synthesis and quantitative reverse transcription PCR

Among the 14 treatments, 8 were used for further qPCR gene expression analyses: -N (1), $+NO_3^-$ (2), -N +NAA (0.01 µM) (7), $+NO_3^-$ +PCIB (5), -N +NAA (0.01 µM) +PCIB (8), -N +TIS108 (3), $+NO_3^-$ +GR24 (4), $+NO_3^-$ +GR24 +NAA (0.01 µM) (6). After 24 h in the equivalent treatment, each whole root was sampled from 4 pooled seedlings for treatment, in three independent biological repetitions, and immediately frozen in liquid nitrogen. Total RNA was extracted as previously described and was reverse transcribed to cDNA as described by Manoli et al. (2012). qRT-PCR was performed using the StepOne Real-Time PCR System (Applied Biosystems, Thermo Fisher Scientific, Waltham, MA USA) as described by Nonis et al. (2007). SYBR Green reagent (Applied Biosystems, Thermo Fisher Scientific, Waltham, MA USA) was used in the reaction, according to the manufacturer's instructions. Melting-curve analysis confirmed the absence of multiple products and primer dimers. Target gene relative expression was determined according to the Livak and Schmittgen (2001) method, using *MEP* (membrane protein PB1A10.07c, Zm00001d018359) as reference gene, according to Manoli et al. (2012). *CCD8* (Zm00001d043442) and *WBC33* (Zm00001d019398) expressions were assessed as key genes for SLs biosynthesis and transport, according to Ravazzolo et al. (2019). Primers were designed using Primer3 web tool (version 4.1.0; https://primer3.ut.ee/ Rozen and Skaletsky, 2000; Untergasser et al. 2012). ANOVA was performed as statistical analysis with significance set with $p < 0.05$ using the web tool SATQPCR (http://satqpcr.sophia.inra.fr/cgi/home.cgi) (Rancurel et al. 2019). SATQPCR results are provided in **Supplementary Table S5**. The list of genes and of primers used are reported in **Supplementary Table S6.**

Phelipanche ramosa *germination bioassay*

Root exudates were collected as reported by Ravazzolo et al. (2019) and used to test the induction of germination in *Phelipanche ramosa* seeds (kindly provided by prof. Giulia Conversa, University of Foggia). After the preconditioning period (Pouvreau et al. 2013), every GFFP (Glass Fiber Filter Paper) disk with parasitic seeds was treated with 50 µL of root exudates, incubated in darkness at 25°C for 6 days and stained with 40 µL of Neutral Red solution (1:4000, w/v) (Guillotin et al. 2016). Germinated seeds were then counted using a stereomicroscope (Olympus BX50 microscope, Olympus Corporation, Tokyo, Japan). Images were captured with an Axiom Zeiss MRc5 colour camera (Carl Zeiss, Oberkochen, Germany), and processed with Gnu Image Manipulation Program (GIMP). Three biological replicates for each treatment and an ANOVA statistic test were performed (n=30). The germination rate was expressed as mean percentage and water was used as a negative control.

Funding

This work was supported by the University of Padova (DOR: 2018, 2019) and by a Ph.D grant from Fondazione Cassa di Risparmio di Padova e Rovigo (CARIPARO 2015). The IJPB benefits from the support of Saclay Plant Sciences-SPS (ANR-17-EUR-0007)

Disclosures

Conflicts of interest: No conflicts of interest declared.

Acknowledgements

This work has benefited from the support of IJPB's Plant Observatory technological platforms.

References

Abe, S., Sado, A., Tanaka, K., Kisugi, T., Asami, K., Ota, S., et al. (2014) Carlactone is converted to carlactonoic acid by MAX1 in Arabidopsis and its methyl ester can directly interact with AtD14 in vitro. *Proc. Natl. Acad. Sci. USA* 111: 18084–18089.

Alarcón, M. V., Salguero, J., & Lloret, P. G. (2019) Auxin Modulated Initiation of Lateral Roots Is Linked to Pericycle Cell Length in Maize. *Frontiers in plant science* 10: 11.

Alarcón, M. V., & Salguero, J. (2017) Transition zone cells reach G2 phase before initiating elongation in maize root apex. *Biology open* 6: 909–913.

Andrews, S. (2010) FastQC A Quality Control tool for High Throughput Sequence Data. Retrieved from http://www.bioinformatics.babraham.ac.uk/projects/fastqc/.

Arite, T., Iwata, H., Ohshima, K., Maekawa, M., Nakajima, M., Kojima, M., et al. (2007) DWARF10, an RMS1/MAX4/DAD1 ortholog, controls lateral bud outgrowth in rice. *Plant J*. 51: 1019–1029.

Atkinson, J.A., Rasmussen, A., Traini, R., Voß, U., Sturrock, C., Mooney, S.J., et al. (2014) Branching out in roots: uncovering form, function, and regulation. *Plant Physiol*. 166: 538-550.

Bainbridge, K., Sorefan, K., Ward, S. and Leyser, O. (2005) Hormonally controlled expression of the Arabidopsis *MAX4* shoot branching regulatory gene. *Plant J.* 44: 569–580.

Benková, E., Michniewicz, M., Sauer, M., Teichmann, T., Seifertová, D., Jürgens, G., et al. (2003) Local, efflux-dependent auxin gradients as a common module for plant organ formation. *Cell* 115: 591–602.

Bolger, A.M.; Lohse, M.; Usadel, B. (2014) Trimmomatic: A flexible trimmer for Illumina sequence data. *Bioinformatics* 30: 2114–2120

Bouguyon, E., Gojon, A. and Nacry, P. (2012) Nitrate sensing and signalling in plants. *Semin. Cell Dev. Biol*. 23: 648–654.

Boutet-Mercey, S., Perreau, F., Roux, A., Clavé, G., Pillot, J.P., Schmitz-Afonsom, I., et al. (2018) Validated method for strigolactone quantification by Ultra High-Performance Liquid Chromatography - Electrospray Ionisation Tandem Mass Spectrometry using novel deuterium labelled standards. *Phytochem Anal.* 1: 59-68.

Charnikhova, T.V., Gaus. K., Lumbroso, A., Sanders, M., Vincken, J.P., De Mesmaeker, A., et al. (2017) Zealactones. Novel natural strigolactones from maize. *Phytochemistry* 137: 123-131.

Du, Y. and Scheres, B. (2018) Lateral root formation and the multiple roles of auxin. *J. Exp. Bot*. 69: 155–167.

Du, Y. and Scheres, B. (2017) PLETHORA transcription factors orchestrate de novo organ patterning during Arabidopsis lateral root outgrowth. *Proc. Natl. Acad. Sci.* 114: 201714410.

Forde, B. (2014) Nitrogen signalling pathways shaping root system architecture: an update. *Curr. Opin. Plant Biol.* 21: 30-36.

Gojon, A. (2017) Nitrogen nutrition in plants: rapid progress and new challenges. *J. Exp. Bot.* 68: 2457–2462.

Guan, J.C., Koch, K.E., Suzuki, M., Wu, S., Latshow, S., Petruff T., et al. (2012) Diverse roles of strigolactone signaling in maize architecture and the uncoupling of a branching-specific subnetwork. *Plant Physiol*. 160: 1303–1317.

Guillotin, B., Etemadi, M., Audran, C., Bouzayen, M., Bécard, G. and Combier, J.P. (2016) Sl-IAA27 regulates strigolactone biosynthesis and mycorrhization in tomato (var. MicroTom). *New Phytol*. 213: 1124–1132.

Hachiya, T. and Sakakibara H. (2017) Interactions between nitrate and ammonium in their uptake, allocation, assimilation, and signaling in plants. *J. Exp. Bot*. 68: 2501-2512.

Hayward, A., Stirnberg, P., Beveridge, C. and Leyser, O. (2009) Interactions between auxin and strigolactone in shoot branching control. *Plant Physiol*. 151:400–412

Hirel B. and Lea, P.J. (2018) Genomics of Nitrogen Use Efficiency in Maize: From Basic Approaches to Agronomic Applications. In: Bennetzen J, Flint-Garcia S, Hirsch C, Tuberosa R (Eds.). *The Maize Genome-Compendium of Plant Genomes*, 259-286.

Hochholdinger, F. and Tuberosa, R. (2009) Genetic and genomic dissection of maize root development and architecture. *Curr. Opin. Plant Biol.* 12: 172–177.

Hu, Y., Xie, Q., & Chua, N. H. (2003) The Arabidopsis auxin-inducible gene ARGOS controls lateral organ size. *The Plant cell*, 15: 1951–1961.

Iqbal A., Qiang, D., Alamzeb, M., Xiangrru, W., Huiping, G., Hehgheng, Z., et al. (2020) Untangling the molecular mechanisms and functions of nitrate to improve nitrogen use efficiency. *J. Sci. Food Agric*. 100: 904–914.

Ito, S., Umehara, M., Hanada, A., Kitahata, N., Hayase, H., Yamaguchi, S., et al. (2011) Effects of triazole derivatives on strigolactone levels and growth retardation in rice. *PLoS One* 6: e21723.

Jansen, L., Hollunder, J., Roberts, I., Forestan, C., Fonteyne, P., Van Quickenborne, C., et al. (2013) Comparative transcriptomics as a tool for the identification of root branching genes in maize. *Plant Biotechnol. J*. 11: 1092–1102.

Jiao, Y.; Peluso, P.; Shi, J.; Liang, T.; Stitzer, M.C.; Wang, B.; Campbell, M.S.; Stein, J.C.; Wei, X.; Chin, C.S.; et al. (2017) Improved maize reference genome with single-molecule technologies. *Nature* 546: 524–52

Kant, S., Bi, Y.M. and Rothstein, S.J. (2011) Understanding plant response to nitrogen limitation for the improvement of crop nitrogen use efficiency. *J. Exp. Bot.* 62: 1499–1509.

Kant, S. (2018) Understanding nitrate uptake, signaling and remobilisation for improving plant nitrogen use efficiency. *Semin Cell Dev Biol*. 74: 89-96.

Kim, D.; Pertea, G.; Trapnell, C.; Pimentel, H.; Kelley, R.; Salzberg, S.L. (2013) TopHat2: Accurate alignment of transcriptomes in the presence of insertions, deletions and gene fusions. *Genome Biol* 14: R36.

Koltai, H., Dor, E., Hershenhorn, J., Joel, D.M., Weininger, S., Lekalla, H.S., et al. (2010) Strigolactones' effect on root growth and root-hair elongation may be mediated by auxin-efflux carriers. *J. Plant Growth Regul*. 29: 129–136.

Koren, D., Resnick, N., Mayzlish Gati, E., Belausov, E., Weininger, S., Kapulnik, Y. and Koltai, H. (2013) Strigolactone signaling in the endodermis is sufficient to restore root responses and involves SHORT HYPOCOTYL 2 (SHY2) activity. *New Phytol.* 198: 866–874.

Kumar, M., Pandya-Kumar, N., Kapulnik, Y. and Koltai, H. (2015) Strigolactone signaling in root development and phosphate starvation. *Plant Signal Behav.* 10: e1045174.

Li, T., Kang, X., Lei, W., Yao, X., Zou, L., Zhang, D., & Lin, H. (2020) SHY2 as a node in the regulation of root meristem development by auxin, brassinosteroids, and cytokinin. *Journal of integrative plant biology* 62: 1500–1517.

Li, H., Hu, B. and Chu, C. (2017) Nitrogen use efficiency in crops: lessons from Arabidopsis and rice. *J. Exp. Bot* 68: 2477-2488.

Li, H.; Handsaker, B.; Wysoker, A.; Fennell, T.; Ruan, J.; Homer, N.; Marth, G.; Abecasis, G.; Durbin, R. (2009) 1000 Genome Project Data Processing Subgroup. The Sequence Alignment/Map format and SAMtools. *Bioinformatics* 25: 2078–2079.

Liang, Y., Ward, S., Li, P., Bennett, T. and Leyser, O. (2016) SMAX1-LIKE7 signals from the nucleus to regulate shoot development in Arabidopsis via partially EAR motif-independent mechanisms. *Plant Cell* 28: 1581–1601.

Liao, Y., Smyth, G.K., and Shim W. (2019) The R package R subread is easier, faster, cheaper and better for alignment and quantification of RNA sequencing reads. *Nucleic Acids Research* 47: e47.

Liao, Y., Smyth, G.K. and Shi, W. (2014) featureCounts: an efficient general-purpose program for assigning sequence reads to genomic features. *Bioinformatics* 30: 923-930.

Ligerot, Y., de Saint Germain, A., Waldie, T., Troadec, C., Citerne, S., Kadakia, N., et al. (2017) The pea branching *RMS2* gene encodes the PsAFB4/5 auxin receptor and is involved in an auxin-strigolactone regulation loop. *PLoS Genet* 13: e1007089.

Livak, K.J. and Schmittgen, T.D. (2001) Analysis of relative gene expression data using real-time quantitative PCR and the $2(-\Delta\Delta C^{(T)})$ method. *Methods* 25: 402–408.

Love, M.I., Huber, W., Anders, S. (2014). Moderated estimation of fold change and dispersion for RNA-seq data with DESeq2. *Genome Biology* 15: 550.

Ludwig, Y., Zhang, Y. and Hochholdinger, F. (2013) The maize (*Zea mays* L.) *AUXIN/INDOLE-3-ACETIC ACID* gene family: phylogeny, synteny, and unique root-type and tissue-specific expression patterns during development. *PLoS One.* 8: e78859.

MacLeod, R.D., Thompson, A. (1979) Development of lateral root primordia in *Vicia faba*, *Pisum sativum*, *Zea mays* and *Phaseolus vulgaris*: Rates of primordium formation and cell doubling times. Ann. Bot. (Lond.) 44: 435–449.

Mandadi, K.K., Misra, A., Ren, S., McKnight, T.D. (2009) BT2, a BTB protein, mediates multiple responses to nutrients, stresses, and hormones in Arabidopsis. *Plant Physiol* 150: 1930–1939.

Manoli, A., Trevisan, S., Voigt, B., Yokawa, K., Baluška, F. and Quaggiotti S. (2016) Nitric Oxide-mediated maize root apex response to nitrate are regulated by auxin and strigolactones. *Front Plant Sci.* 6: 1269.

Manoli, A., Begheldo, M., Genre, A., Lanfranco, L., Trevisan, S. and Quaggiotti S. (2014) NO homeostasis is a key regulator of early nitrate perception and root elongation in maize. *J Exp Bot*. 65: 185-200.

Manoli, A., Sturaro, A., Trevisan, S., Quaggiotti, S. and Nonis, A. (2012) Evaluation of candidate reference genes for qPCR in maize. *J Plant Physiol* 169: 807–815.

Martínez-de la Cruz, E., García-Ramírez, E., Vázquez-Ramos, J.M., Reyes de la Cruz, H. and López-Bucio, J. (2015) Auxins differentially regulate root system architecture and cell cycle protein levels in maize seedlings. *J Plant Physiol*. 176: 147-156.

Marzec, M. and Melzer, M. (2018) Regulation of Root Development and Architecture by Strigolactones under Optimal and Nutrient Deficiency Conditions. *Int. J. Mol. Sci*. 19: 1887.

Matusova, R., Rani, K., Verstappen, F.W.A., Franssen, M.C.R., Beale, M.H., and Bouwmeester, H.J. (2005) The strigolactone germination stimulants of the plant-parasitic Striga and Orobanche spp. are derived from the carotenoid pathway. *Plant Physiol.* 139: 920–934.

Miller, A.J. and Cramer, M.D. (2004) Root Nitrogen Acquisition and Assimilation. *Plant Soil* 274: 1-36.

Mounier, E., Pervent, M., Ljung, K., Gojon, A. and Nacry, P. (2014) Auxin-mediated nitrate signalling by NRT1.1 participates in the adaptive response of Arabidopsis root architecture to the spatial heterogeneity of nitrate availability. *Plant Cell Environ*. 37: 162–174.

Nieto-Sotelo, J., Martínez, L. M., Ponce, G., Cassab, G. I., Alagón, A., Meeley, R. B., Ribaut, J. M., & Yang, R. (2002). Maize HSP101 plays important roles in both induced and basal thermotolerance and primary root growth. *The Plant cell*, 14: 1621–1633.

Nishimura, T., Nakano, H., Hayashi, K., Niwa, C., Koshiba, T. (2009). Differential downward stream of auxin synthesized at the tip has a key role in gravitropic curvature via TIR1/AFBs-mediated auxin signaling pathways. *Plant and Cell Physiology* 50: 1874–1885.

Nonis, A., Ruperti, B., Falchi, R., Casatta, E., Thamashebi, S.E. and Vizzotto, G. (2007) Differential expression and regulation of a neutral invertase encoding gene from peach (*Prunus persica):* evidence for a role in fruit development. *Physiol Plant* 129: 436-446.

Oono, Y., Ooura, C., Rahman, A., Aspuria, E.T., Hayashi, K., Tanaka, A. and Uchimiya, H. (2003) p-Chlorophenoxyisobutyric acid impairs auxin response in Arabidopsis root. *Plant Physiol*. 133: 1135–1147.

Plett, D.C., Holtham, L.R., Okamoto, M. and Garnett, T.P. (2018) Nitrate uptake and its regulation in relation to improving nitrogen use efficiency in cereals. *Semin. Cell Dev. Biol*. 74: 97–104.

Pouvreau, J.B., Gaudin, Z., Auger, B., Lechat, M.M., Gauthier, M., Delavault, P., et al. (2013) A high-throughput seed germination assay for root parasitic plants. *Plant Methods* 9: 32.

Prusinkiewicz, P., Crawford, S., Smith, R.S., Ljung, K., Bennett, T., Ongaro, V. and Leyser, O. (2009) Control of bud activation by an auxin transport switch. *Proc. Natl. Acad. Sci. U S A* 106: 17431–17436.

Rameau, C., Goormachtig, S., Cardinale, F., Bennett, T. and Cubas P. (2019) Strigolactones as Plant Hormones. In: Koltai H., Prandi C. (eds) *Strigolactones - Biology and Applications*. Springer, Cham.

Rancurel, C., Van Tran, T., Elie, C., & Hilliou, F. (2019). SATQPCR: Website for statistical analysis of real-time quantitative PCR data. *Molecular and cellular probes* 46: 101418.

Ravazzolo, L., Trevisan, S., Manoli, A., Boutet-Mercey, S., Perreau, F. and Quaggiotti, S. (2019) The control of zealactone biosynthesis and exudation is involved in the response to nitrogen in maize root. *Plant Cell Physiol*. 60: 2100-2112.

Ren, S., Mandadi, K.K., Boedeker, A.L., Rathore, K.S. and McKnight, T.D. (2007) Regulation of telomerase in Arabidopsis by BT2, an apparent target of TELOMERASE ACTIVATOR1. *Plant Cell*, 19, 23–31.

Robert, H. S., Quint, A., Brand, D., Vivian-Smith, A., & Offringa, R. (2009) BTB and TAZ domain scaffold proteins perform a crucial function in Arabidopsis development. *The Plant journal: for cell and molecular biology* 58: 109–121.

Rozen, S. and Skaletsky, H. (2000) Primers3 on the WWW for general users and for biologist programmers. *Methods Mol Biol* 132: 365-386.

Ruyter-Spira, C., Kohlen, W., Charnikhova, T., van Zeijl, A., van Bezouwen, L., de Ruijter N., et al. (2011) Physiological effects of the synthetic strigolactone analog GR24 on root system architecture in Arabidopsis: another belowground role for strigolactones? *Plant Physiol* 155: 721–734.

Shi, J., Drummond, B. J., Wang, H., Archibald, R. L., & Habben, J. E. (2016). Maize and Arabidopsis ARGOS Proteins Interact with Ethylene Receptor Signaling Complex, Supporting a Regulatory Role for ARGOS in Ethylene Signal Transduction. *Plant physiology*, *171*(4), 2783–2797.

Shinohara, N., Taylor, C. and Leyser, O. (2013) Strigolactone can promote or inhibit shoot branching by triggering rapid depletion of the auxin efflux protein PIN1 from the plasma membrane. *PLoS Biol* 11: e1001474.

Smith, S. and De Smet, I. (2012) Root system architecture: insights from *Arabidopsis* and cereal crops. *Philos. Trans. R. Soc. B.* 367: 1441–1452.

Soundappan, I., Bennett, T., Morffy, N., Liang, Y., Stanga, J.P., Abbas A., et al. (2015) SMAX1-LIKE/D53 family members enable distinct MAX2-dependent responses to strigolactones and karrikins in Arabidopsis. *Plant Cell* 27: 3143–3159.

Sun, H., Tao, J., Liu S., Huang, S., Chen, S., Xie X., et al. (2014) Strigolactones are involved in phosphate- and nitrate-deficiency-induced root development and auxin transport in rice. *J Exp Bot* 65: 6735–6746.

Sun, C.H., Yu, J.Q. and Hu, D.G. (2017) Nitrate: A Crucial Signal during Lateral Roots Development. *Front Plant Sci*. 8: 485.

Sun, H., Xu, F., Guo, X., Wu, D., Zhang, X., Lou, M., et al. (2019a) A Strigolactone Signal Inhibits Secondary Lateral Root Development in Rice. *Front. Plant Sci*. 10: 1527.

Sun, L., Dong, S., Ge, Y., Fonseca, J. P., Robinson, Z. T., Mysore, K. S., & Mehta, P. (2019b). DiVenn: An Interactive and Integrated Web-Based Visualization Tool for Comparing Gene Lists. *Frontiers in genetics* 10: 421.

Tai, H., Lu, X., Opitz, N., Marcon, C., Paschold, A., Lithio, A., et al. (2016) Transcriptomic and anatomical complexity of primary, seminal, and crown roots highlight root type-specific functional diversity in maize (*Zea mays* L.). *J. Exp. Bot*. 67: 1123–1135.

Tian, H., De Smet I. and Ding Z. (2014) Shaping a root system: regulating lateral versus primary root growth. *Trends Plant Sci.* 19: 426–431.

Trevisan, S., Manoli, A., Ravazzolo, L., Botton, A., Pivato, M., Masi, A. and Quaggiotti, S. (2015) Nitrate sensing by the maize root apex transition zone: a merged transcriptomic and proteomic survey. *J. Exp. Bot.* 66: 3699-3715.

Umehara, M., Hanada, A., Magome, H., Takeda-Kamiya, N. and Yamaguchi, S. (2010) Contribution of strigolactones to the inhibition of tiller bud outgrowth under phosphate deficiency in rice. *Plant Cell Physiol* 51: 1118–1126.

Undurraga, S.F., Ibarra-Henríquez, C., Fredes, I., Álvarez, J.M. and Gutiérrez, R.A. (2017) Nitrate signaling and early responses in Arabidopsis roots. *J. Exp Bot.* 68: 2541-2551.

Untergasser, A., Cutcutache, I., Koressaar, T., Ye, J., Faircloth, B.C., Remm, M. and Rozen, S.G. (2012) Primer3-new capabilities and interfaces. *Nucleic Acids Res*. 40: e115.

Vidal, E.A., Moyano, T.C., Riveras, E., Contreras-López, O. and Gutiérrez, R.A. (2013) Systems approaches map regulatory networks downstream of the auxin receptor AFB3 in the nitrate response of *Arabidopsis thaliana* roots. *Proc. Natl. Acad. Sci. USA*. 110: 12840–12845.

Wang, Y.Y., Cheng, Y.H., Chen, K.E. and Tsay, Y.F. (2018) Nitrate Transport, Signaling, and Use Efficiency. *Annu Rev Plant Biol*. 69: 85-122.

Willemsen, V., Bauch, M., Bennett, T., Campilho, A., Wolkenfelt, H., Xu, J., Haseloff, J., & Scheres, B. (2008). The NAC domain transcription factors FEZ and SOMBRERO control the orientation of cell division plane in Arabidopsis root stem cells. *Developmental cell* 15: 913–922.

Xu, P. and Cai, W. (2019) Nitrate-responsive OBP4-XTH9 regulatory module controls lateral root development in *Arabidopsis thaliana*. *PLoS Genet* 15: e1008465.

Xuan, W., Beeckman, T. and Guohua, X. (2017) Plant nitrogen nutrition: sensing and signalling. *Curr. Opin. Plant Biol.* 39: 57-65.

Yu, P., White, P.J. and Li, C. (2015) New insights to lateral rooting: Differential responses to heterogeneous nitrogen availability among maize root types. *Plan Signal. Behav*. 10: e1013795.

Yu, P., Baldauf, J.A., Lithio, A., Marcon, C., Nettleton, D., Li, C. and Hochholdinger, F. (2016) Root Type-Specific Reprogramming of Maize Pericycle Transcriptomes by Local High Nitrate Results in Disparate Lateral Root Branching Patterns. *Plant Physiol.* 170: 1783-1798.

Yu, P., Marcon, C., Baldauf, J.A., Frey, F., Baer, M. and Hochholdinger, F. (2018) Transcriptomic dissection of maize root system development. In: Bennetzen J., Flint-Garcia S., Hirsch C., Tuberosa R. (eds) *The Maize Genome. Compendium of Plant Genomes*. Springer, Cham.

Yu, P., Hochholdinger, F. and Li, C. (2019) Plasticity of Lateral Root Branching in Maize. *Front Plant Sci*. 10: 363.

Zhang, X., Cui, Y., Yu, M., Su, B., Gong, W., Baluška, F., et al. (2019) Phosphorylation-Mediated Dynamics of Nitrate Transceptor NRT1.1 Regulate Auxin Flux and Nitrate Signaling in Lateral Root Growth. *Plant Physiol*. 181: 480–498.

Zhang H. and Forde B.G. (2000) Regulation of Arabidopsis root development by nitrate availability. *J. Exp. Bot.* 1: 51–59.

Zwanenburg, B., Zeljković, S., Pospíšil, T. (2016) Synthesis of strigolactones, a strategic account. *Pest Manag Sci*. 72:15-29.

Tables

Table 1: List of treatments used in the study. Abbreviations: PA, phenotypical analysis; RNA-seq, RNA-sequencing; qPCR, Real-time PCR.

ID	Treatment description	Aim of the treatment	Analysis performed
1	-N	nitrogen-deprived nutrient solution (**negative control**)	PA; RNA-seq; qPCR
2	$+NO_3^-$ (1 mM)	nitrate-supplied nutrient solution (**positive control**)	PA; RNA-seq; qPCR
3	$+NO_3^-$ (1 mM) +PCIB (10 µM)	inhibition of auxin signalling	PA; RNA-seq; qPCR
4	-N+NAA (0.01 µM)	provision of a synthetic auxin	PA; qPCR
5	-N+NAA (0.05 µM)	provision of a synthetic auxin	PA;
6	-N+NAA (0.1 µM)	provision of a synthetic auxin	PA;
7	-N+NAA (1 µM)	provision of a synthetic auxin	PA;
8	-N+NAA (0.01 µM) +PCIB (10 µM)	provision of a synthetic auxin but inhibition of auxin signalling	PA; qPCR
9	$+NO_3^-$ (1 mM) +GR24 (2 µM)	provision of a synthetic strigolactone analogue	PA; qPCR
10	$+NO_3^-$ (1 mM) +GR24 (2 µM) +NAA (0.01 µM)	provision of a synthetic strigolactone analogue and of a synthetic auxin	PA; qPCR
11	$+NO_3^-$ (1 mM) +GR24 (2 µM) +NAA (0.05 µM)	provision of a synthetic strigolactone analogue and of a synthetic auxin	PA;
12	$+NO_3^-$ (1 mM) +GR24 (2 µM) +NAA (0.1 µM)	provision of a synthetic strigolactone analogue and of a synthetic auxin	PA;
13	-N +TIS108 (2 µM)	inhibition of strigolactones biosynthesis	PA; RNA-seq; qPCR
14	-N +TIS108 (2 µM) +PCIB (10 µM)	inhibition of strigolactones biosynthesis and of auxin signalling	PA;

Figure legends

Figure 1. SL quantification on root tissue. Quantitative analysis of the relative amounts of putative zealactone forms (A) and putative carlactonoic acid (B) in maize root tissues [in percentage, as normalized relative to average N-starvation amount per fresh weight] of seedlings exposed to additional 24h of nitrate ($+NO_3^-$) or N-starvation (-N) after a 24h-pre-incubation under N-deficient conditions. Quantification in root tissues of phosphate-starved seedlings (-P) was included as positive control. The root tissues were collected after 24 h of each treatment and immediately shock-frozen in liquid nitrogen. Following addition of GR24 as an internal standard and extraction, the analytes were quantified by LC-MS/MS, MRM mode, as described by Ravazzolo et al. (2019). Values are mean ± SE of three replicates. n.d.: non-detected.

Figure 2. Lateral root primordia (LRP) density of maize seedlings exposed to different nitrogen provision and different auxin and SL inhibitors and analogue. Maize seedlings were grown for 24 hours in a N-deprived nutrient solution and then transferred for additional 24 hours to different treatments, as reported in **Table 1**: N-deprived solution, 1 mM nitrate-supplied media, nitrate-supplied solution with 10 µM PCIB, N-deprived solution supplied with 0.01 µM NAA; N-deprived solution supplied with 0.01 µM NAA and 10 µM PCIB; nitrate-supplied solution with 2 µM GR24; nitrate-supplied solution with 2 µM GR24 and 0.01 µM NAA; N-deprived solution supplied with 2 µM TIS108; N-deprived solution supplied with 2 µM TIS108 and 10 µM PCIB. A haematoxylin staining was used to evidence the lateral root primordia (LRP) as described by Ravazzolo et al. (2019). Root images were collected using a flatbed scanner and analysed using the ImageJ Software. Data are expressed as increment of LRP density respect to the positive control of nitrate-supplied plants. Red line represents the threshold of the negative control (-N). Results are presented as mean ± SE from three biological replicates for each treatment and an ANOVA statistic test was performed (n=30). Letters next to the bars indicate different significance groups ($P<0.05$).

Figure 3. Real-time qRT-PCR expression profiles of SL marker genes (*CCD8*, *WBC33*) in maize roots (A-B) and *Phelipanche ramosa* germination bioassay by root exudates of maize seedlings (C). For gene expression analysis (panel A-B), maize seedlings were grown 24 hours in a N-deprived nutrient solution and then transferred for additional 24 hours to the different treatments with auxin and strigolactones (SLs) analogues e/o inhibitors, as reported in Table 1**.** After 24 h of each treatment, the complete root system was collected from every seedling (n=4) and the relative mRNA levels for each gene were evaluated by means of qRT-PCR. Data are mean ± SE for three biological replicates. In panel C, maize seedlings were grown 24 hours in a N-deprived nutrient solution and then transferred to a 1mM nitrate-supplied media ($+NO_3^-$), to a N-deprived solution (-N) or to a N-deprived solution supplied with 0.01 µM NAA (-N+NAA 0.01) or to a N-deprived solution supplied with TIS108 2 µM (-N+TIS108) or to a nitrate-supplied media plus GR24 2 µM ($+NO_3^-$ +GR24) for additional 24 hours. Root exudates were collected as reported by Pouvreau et al. (2013) and used to test the induction of germination in *Phelipanche ramosa* seeds. Each disk was treated with root exudates in triplicate. Germinated seeds were evidenced by Neutral Red staining and counted using a stereo microscope. The germination rate was expressed as mean percentage and water was used as negative control.

Figure 4. Distribution of differentially expressed genes (DEGs) identified by RNA-seq analysis with log2 FC >|1| and FDR ≤ 0.05 for NO_3^-/-N treatment (A), and log2 FC >|0.58| and FDR ≤ 0.05 for other pairwise comparisons (-N+TIS108/-N; -N+TIS108/+NO_3^-; +NO_3^-+PCIB/-N; +NO_3^-+PCIB/+NO_3^-) (B). Panel A summarizes genes up- or down-regulated by nitrate provision with respect to -N, grouped basing on the magnitude of their transcriptional changes. The Venn diagram (B) shows the numerical comparison of all significant up- and down-regulated differential expressed genes following $+NO_3^-$ or -N +TIS108 or $+NO_3^-$ +PCIB treatments. The no overlapping numbers represent the genes that are uniquely identified as differentially expressed in the corresponding treatment. The green circles represent significant DEGs in response to nitrate provision and in at least one other treatment (848 DEGs total) which were further analysed.

Figure 5. (A) DEG clusters and their subgroups (when present) based on the similar expression among the $+NO_3^-$ and -N +TIS108 treatments for the TIS108-responsive genes and opposite gene expression among the $+NO_3^-$ and $+NO_3^-$ +PCIB treatments fort the PCIB-responsive genes. Re-scaled expression values for each gene in each sample are reported in a blue to red colour scale (blue: lower FPKM values, red: higher FPKM values). FPKM: Fragments Per Kb per Million. **(B) Pathway assignment based on KEGG mapper reconstruction of DEGs specific of Subgroup of cluster 1 (SL dependent), Cluster 2 (SL/auxin independent), Subgroup of cluster 3 (SL/auxin dependent), and Cluster 4 (auxin-dependent).**

Figure 6. **Realtime gene expression data expressed as an heatmap with hierarchical clustering**. The expression levels of genes are presented using mRNA levels normalized to *MEP* (Zm00001d018359, Manoli et al. 2012) transformed to log2 values in a blue to red colour scale (blue: lower log2 values, red: higher log2 values). Asterisks beyond genes name represents significance codes for ANOVA: *** for p<0.001; ** for p<0.01; * for p< 0.05.

Figure 7. Hypothetical model based on RNA-seq clusterization of how nitrate signalling might control lateral root (LR) development through four independent pathways (A, B, C, D), with the particular involvement of auxin (IAA) and strigolactones (SL). DEGs were clusterized according to RNA-seq results as follow: subgroup of Cluster 1, SL-dependent (TIS108-responsive, PCIB-unresponsive); Cluster 2, SL/auxin independent (unresponsive to both TIS108 and PCIB); subgroup of Cluster 3, SL/auxin dependent (responsive to both TIS108 and PCIB); Cluster 4, auxin-dependent (PCIB-responsive, TIS108-unresponsive). Up arrows indicate induction, down arrows indicate reduction. Genes are indicated in italic. Abbr.: DEGs, Differentially Expressed Genes; FPKM, fragments per kilobase of exon model per million mapped reads; LR, lateral roots; IAA, auxin; SL, strigolactones.

Supplementary data

Supplementary dataset 1: Summary of gene expression values (expressed as fragments per kilobase of exon model per million mapped reads, FPKM) for all treatments tested (-N; $+NO_3^-$; -N +TIS108; $+NO_3^-$ +PCIB)

Supplementary dataset 2: DESeq2 complete results of pairwise differential expression analyses ($+NO_3^-$ vs -N)

Supplementary dataset 3: DESeq2 complete results of pairwise differential expression analyses (-N +TIS108 vs -N)

Supplementary dataset 4: DESeq2 complete results of pairwise differential expression analyses (-N +TIS108 vs $+NO_3^-$)

Supplementary dataset 5: DESeq2 complete results of pairwise differential expression analyses ($+NO_3^-$ +PCIB vs -N)

Supplementary dataset 6: DESeq2 complete results of pairwise differential expression analyses ($+NO_3^-$ +PCIB vs $+NO_3^-$)

Supplementary Table S1: MRM transitions exhibiting a signal for the screening of SLs in root samples. Tr, retention time. In bold, main transition used for quantification.

Supplementary Table S2: Summary statistics of RNA-Seq read sequencing, quality trimming and mapping. For each condition (-N; $+NO_3^-$, -N +TIS108, $+NO_3^-$ +PCIB), three biological replicates were processed (R1, R2, R3).

Supplementary Table S3: Expression matrix of differentially expressed genes (DEGs) showing a log2 fold change ratio >1|and a false discovery rate (FDR)-adjusted p-value ≤ 0.05 in at least one treatment that were included in the hierarchical clustering analysis. FPMK expression values in -N, $+NO_3^-$, -N +TIS108, and $+NO_3^-$ +PCIB samples and clustering results are reported for each of the 848 DEGs.

Supplementary Table S4: Complete KEGG Reconstruction Pathways results for each cluster.

Supplementary Table S5: ANOVA statistical results by means of SATQPCR web tool.

Supplementary Table S6: List of genes and primers used in the study. Abbreviations: n.d. non-detectable.

Supplementary Figure S1: Lateral root primordia (LRP) density of maize seedlings exposed to different nitrogen provision, a SL-analogue (GR24) and different exogenous auxin concentrations as NAA. To choose the most physiological NAA concentration, maize seedlings were grown for 24 hours in a N-deprived nutrient solution and then transferred for additional 24 hours into: N-deprived solution (-N), 1 mM nitrate-supplied media ($+NO_3^-$), N-deprived solution supplied with 0.01 µM NAA (-N +NAA 0.01 µM); N-deprived solution supplied with 0.05 µM NAA (-N +NAA 0.05 µM);); N-deprived solution supplied with 0.1 µM NAA (-N +NAA 0.1 µM); N-deprived solution supplied with 1 µM NAA (-N +NAA 1 µM); nitrate-supplied solution with 2 µM GR24 and 0.01 µM NAA; nitrate-supplied solution with 2 µM GR24 and 0.05 µM NAA; and nitrate-supplied solution with 2 µM GR24 and 0.1 µM NAA. A haematoxylin staining was used to evidence the lateral root primordia (LRP) as described by Ravazzolo et al. (2019). Root images were collected using a flatbed scanner and analysed using the ImageJ Software. Data are expressed as increment of LRP density respect to the positive control ($+NO_3^-$). Results are presented as mean ± SE from three biological replicates for each treatment and an ANOVA statistic test was performed (n=30). Letters above the bars indicate different significance groups ($P<0.05$).

Supplementary Figure S2: Clustering analysis of genes differentially expressed in $+NO_3^-$, -N+TIS108 and $+NO_3^-$ +PCIB treatments with respect to the control (-N) in maize root tissues. z-score scaled FPKM values for all the 848 genes resulted as DEGs in at least one treatment were used for hierarchical clustering analysis. The analysis reveals four different clusters with specific expression behaviours in response to different N-provision or deficiency and SL and auxin inhibitors. Re-scaled expression values for each gene in each sample are reported in a blue to red colour scale (blue: lower FPKM values, red: higher FPKM values). FPKM: Fragments Per Kilobase of exon model per Million mapped reads.

Supplementary Figure S3: Principal Component Analysis (PCA) plot of RNA-seq gene counts showing the grouping of sequenced biological replicates and relationships among samples.

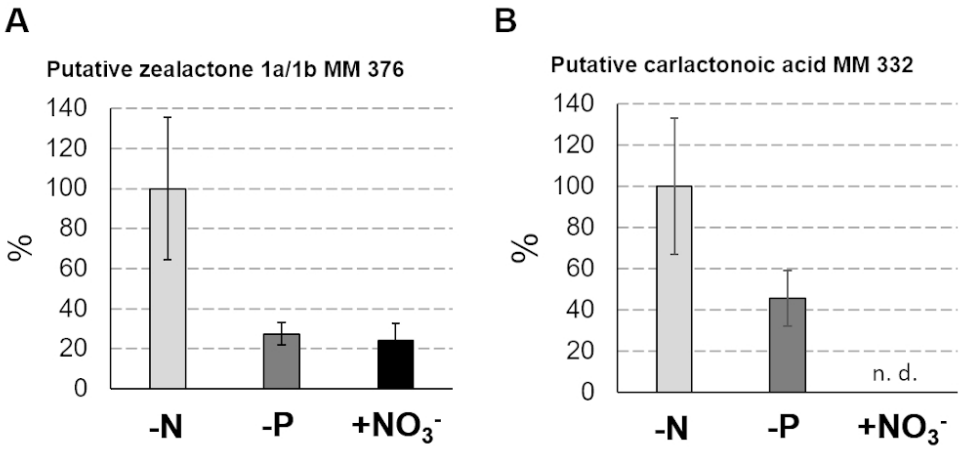

Figure 1. SL quantification on root tissue. Quantitative analysis of the relative amounts of putative zealactone forms (A) and putative carlactonoic acid (B) in maize root tissues [in percentage, as normalized relative to average N-starvation amount per fresh weight] of seedlings exposed to additional 24h of nitrate (+NO3-) or N-starvation (-N) after a 24h-pre-incubation under N-deficient conditions. Quantification in root tissues of phosphate-starved seedlings (-P) was included as positive control. The root tissues were collected after 24 h of each treatment and immediately shock-frozen in liquid nitrogen. Following addition of GR24 as an internal standard and extraction, the analytes were quantified by LC-MS/MS, MRM mode, as described by Ravazzolo et al. (2019). Values are mean ± SE of three replicates. n.d.: non-detected.

86x40mm (300 x 300 DPI)

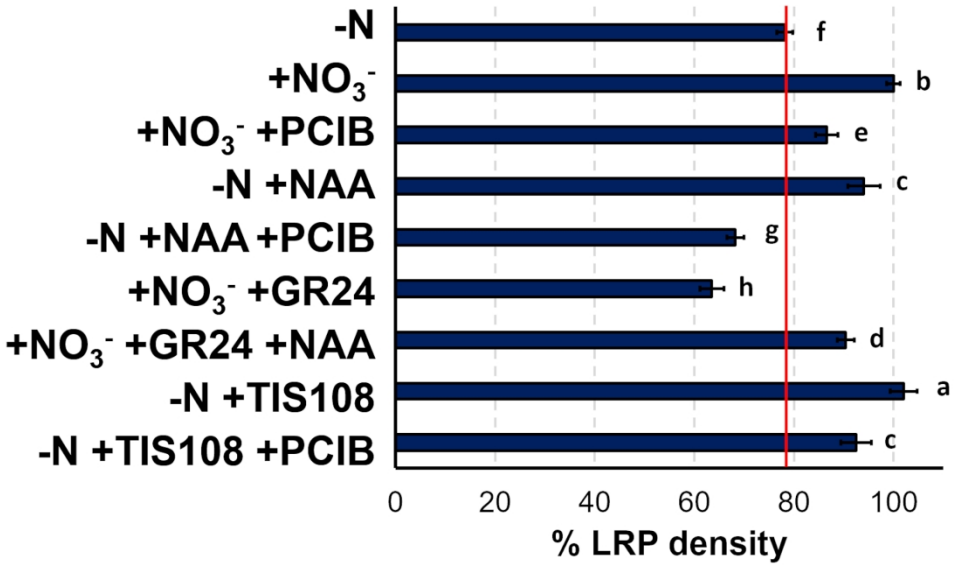

Figure 2. Lateral root primordia (LRP) density of maize seedlings exposed to different nitrogen provision and different auxin and SL inhibitors and analogue. Maize seedlings were grown for 24 hours in a N-deprived nutrient solution and then transferred for additional 24 hours to different treatments, as reported in Table 1: N-deprived solution, 1 mM nitrate-supplied media, nitrate-supplied solution with 10 μM PCIB, N-deprived solution supplied with 0.01 μM NAA; N-deprived solution supplied with 0.01 μM NAA and 10 μM PCIB; nitrate-supplied solution with 2 μM GR24; nitrate-supplied solution with 2 μM GR24 and 0.01 μM NAA; N-deprived solution supplied with 2 μM TIS108; N-deprived solution supplied with 2 μM TIS108 and 10 μM PCIB. A haematoxylin staining was used to evidence the lateral root primordia (LRP) as described by Ravazzolo et al. (2019). Root images were collected using a flatbed scanner and analysed using the ImageJ Software. Data are expressed as increment of LRP density respect to the positive control of nitrate-supplied plants. Red line represents the threshold of the negative control (-N). Results are presented as mean ± SE from three biological replicates for each treatment and an ANOVA statistic test was performed (n=30). Letters next to the bars indicate different significance groups ($P<0.05$).

177x104mm (300 x 300 DPI)

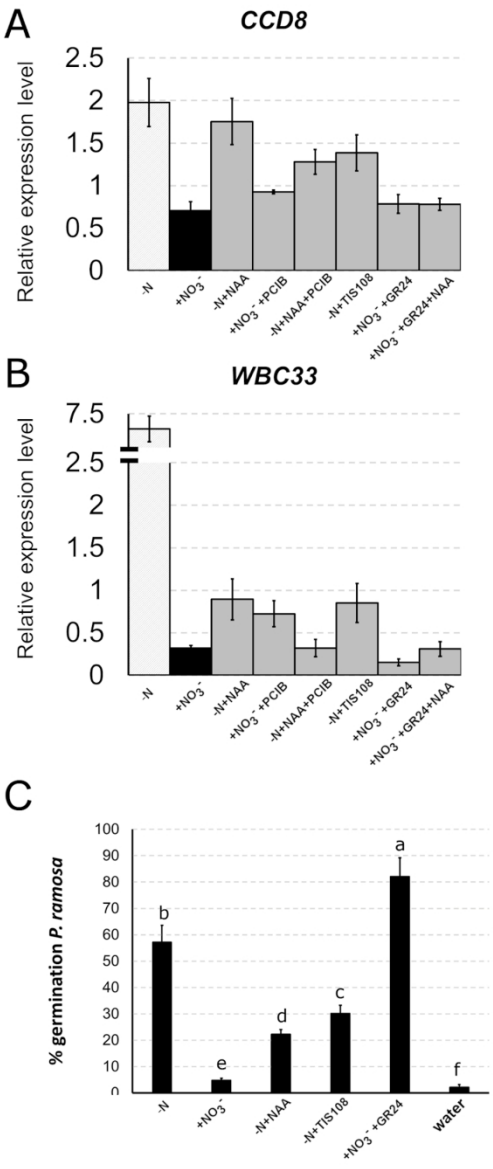

Figure 3. Real-time qRT-PCR expression profiles of SL marker genes (CCD8, WBC33) in maize roots (A-B) and Phelipanche ramosa germination bioassay by root exudates of maize seedlings (C). For gene expression analysis (panel A-B), maize seedlings were grown 24 hours in a N-deprived nutrient solution and then transferred for additional 24 hours to the different treatments with auxin and strigolactones (SLs) analogues e/o inhibitors, as reported in Table 1. After 24 h of each treatment, the complete root system was collected from every seedling (n=4) and the relative mRNA levels for each gene were evaluated by means of qRT-PCR. Data are mean ± SE for three biological replicates. In panel C, maize seedlings were grown 24 hours in a N-deprived nutrient solution and then transferred to a 1mM nitrate-supplied media (+NO3-), to a N-deprived solution (-N) or to a N-deprived solution supplied with 0.01 μM NAA (-N+NAA 0.01) or to a N-deprived solution supplied with TIS108 2 μM (-N+TIS108) or to a nitrate-supplied media plus GR24 2 μM (+NO3- +GR24) for additional 24 hours. Root exudates were collected as reported by Pouvreau et al. (2013) and used to test the induction of germination in Phelipanche ramosa seeds. Each disk was treated with root exudates in triplicate. Germinated seeds were evidenced by Neutral Red staining and counted using a stereo microscope. The germination rate was expressed as mean percentage and water was used as negative

control.

87x203mm (300 x 300 DPI)

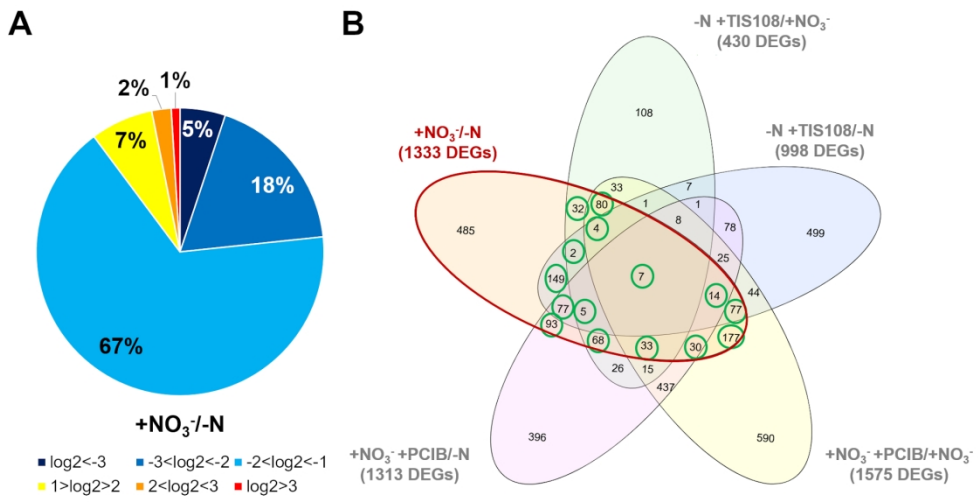

Figure 4. Distribution of differentially expressed genes (DEGs) identified by RNA-seq analysis with log2 FC >|1| and FDR ≤ 0.05 for NO3-/-N treatment (A), and log2 FC >|0.58| and FDR ≤ 0.05 for other pairwise comparisons (-N+TIS108/-N; -N+TIS108/+NO3-; +NO3-+PCIB/-N; +NO3-+PCIB/+NO3-) (B). Panel A summarizes genes up- or down-regulated by nitrate provision with respect to -N, grouped basing on the magnitude of their transcriptional changes. The Venn diagram (B) shows the numerical comparison of all significant up- and down-regulated differential expressed genes following +NO3− or -N +TIS108 or +NO3− +PCIB treatments. The no overlapping numbers represent the genes that are uniquely identified as differentially expressed in the corresponding treatment. The green circles represent significant DEGs in response to nitrate provision and in at least one other treatment (848 DEGs total) which were further analysed.

173x93mm (300 x 300 DPI)

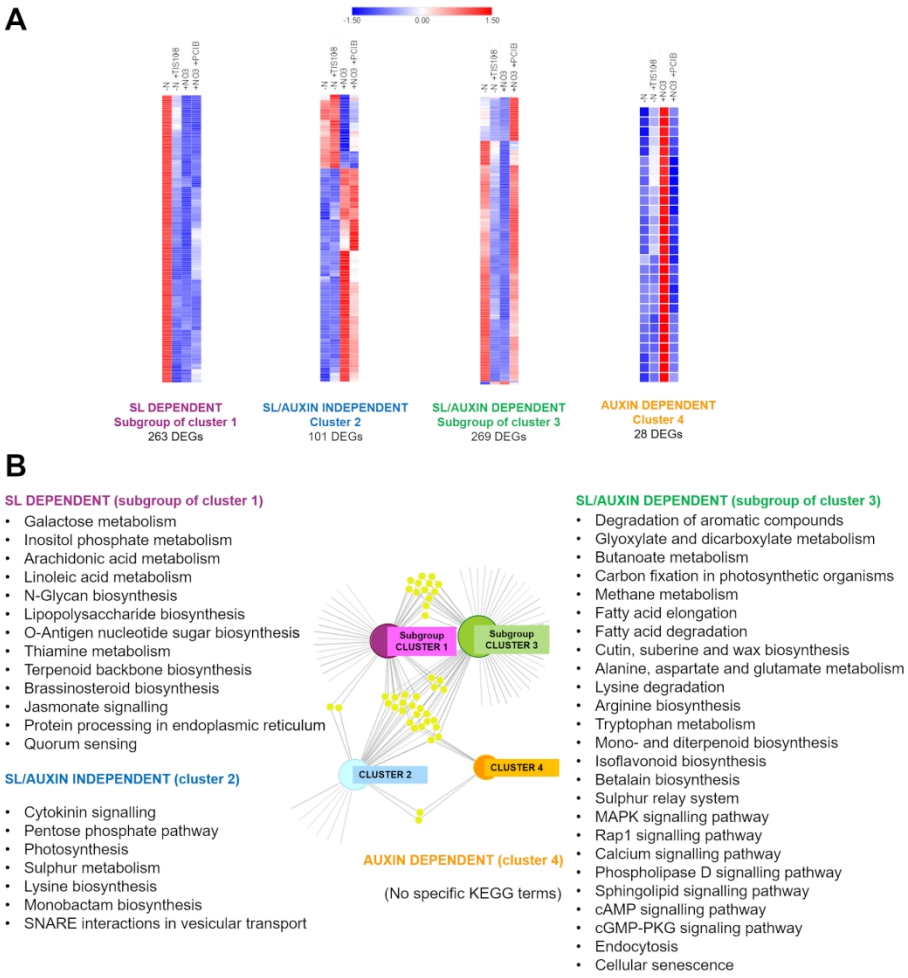

Figure 5. (A) DEG clusters and their subgroups (when present) based on the similar expression among the +NO3- and -N +TIS108 treatments for the TIS108-responsive genes and opposite gene expression among the +NO3- and +NO3- +PCIB treatments fort the PCIB-responsive genes. Re-scaled expression values for each gene in each sample are reported in a blue to red colour scale (blue: lower FPKM values, red: higher FPKM values). FPKM: Fragments Per Kb per Million. (B) Pathway assignment based on KEGG mapper reconstruction of DEGs specific of Subgroup of cluster 1 (SL dependent genes), Cluster 2 (SL/auxin independent), Subgroup of cluster 3 (SL/auxin dependent), and Cluster 4 (auxin-dependent).

173x173mm (300 x 300 DPI)

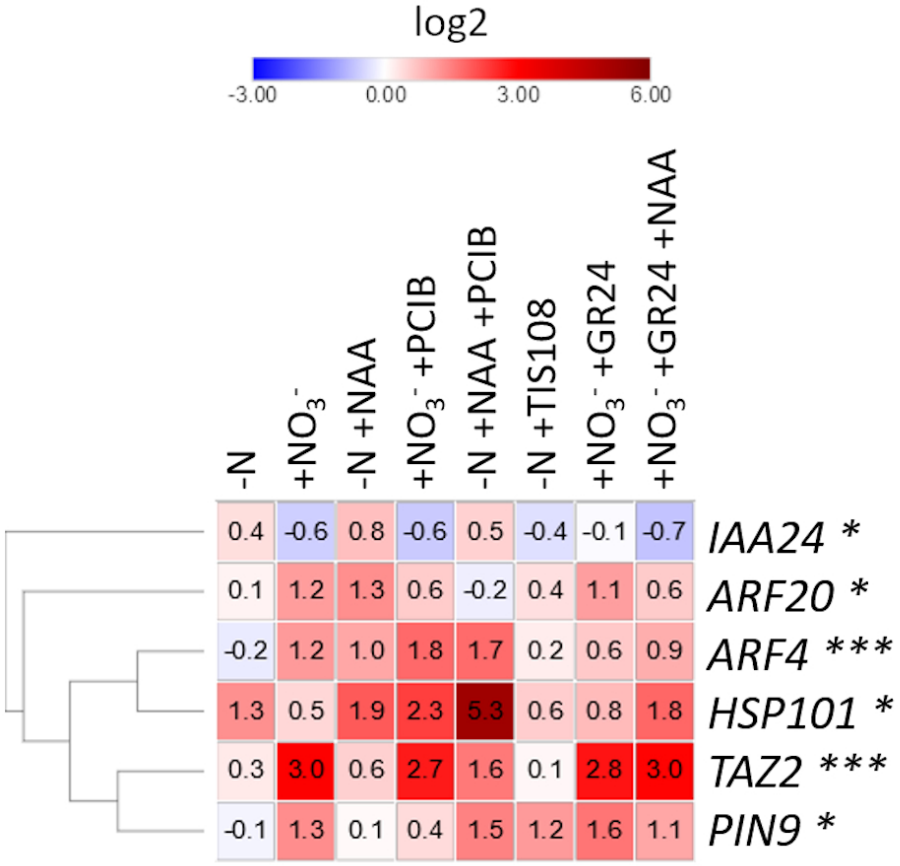

Figure 6. Realtime gene expression data expressed as an heatmap with hierarchical clustering. The expression levels of genes are presented using mRNA levels normalized to MEP (Zm00001d018359, Manoli et al. 2012) transformed to log2 values in a blue to red colour scale (blue: lower log2 values, red: higher log2 values). Asterisks beyond genes name represents significance codes for ANOVA: *** for p<0.001; ** for p<0.01; * for p< 0.05.

86x78mm (300 x 300 DPI)

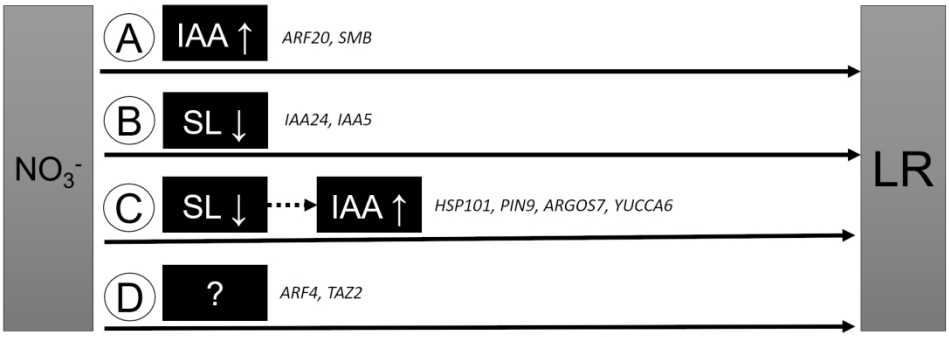

			FPKM				
Gene ID	**Gene description**	**Gene accession**	**-N**	**-N +TIS108**	**+NO_3^-**	**+NO_3^-+PCIB**	**cluster**
IAA24	Auxin-responsive protein, Aux/IAA-transcription factor 24	Zm00001d018973	27.233	15.880	6.258	6.687	1
IAA5	Auxin-responsive protein, Aux/IAA-transcription factor 5	Zm00001d034463	4.182	2.733	1.483	1.093	1
ARF4	Auxin response factor 4	Zm00001d001945	1.895	2.588	5.465	4.232	2
TAZ2	BTB/POZ and TAZ domain-containing protein 2	Zm00001d042443	5.979	6.732	33.141	22.645	2
HSP101	heat-shock protein 101, also called Chaperone protein ClpB1	Zm00001d038806	4.593	2.793	1.285	5.461	3
YUCCA6	indole-3-pyruvate monooxygenase	Zm00001d008255	2.330	1.215	0.661	3.983	3
ARGOS7	Auxin regulated gene involved in organ size 7	Zm00001d016857	8.556	4.670	4.139	10.763	3
PIN9	Auxin efflux carrier component, PIN-formed protein9	Zm00001d043179	2.545	6.056	7.449	5.023	3
ARF20	Auxin response factor 20	Zm00001d015243	6.215	8.733	13.154	6.630	4
SMB	SOMBRERO, NAC-transcription factor 19	Zm00001d016119	2.149	3.868	6.033	2.326	4

Figure 7. Hypothetical model based on RNA-seq clusterization of how nitrate signalling might control lateral root (LR) development through four independent pathways (A, B, C, D), with the particular involvement of auxin (IAA) and strigolactones (SL). DEGs were clusterized according to RNA-seq results as follow: subgroup of Cluster 1, SL-dependent (TIS108-responsive, PCIB-unresponsive); Cluster 2, SL/auxin independent (unresponsive to both TIS108 and PCIB); subgroup of Cluster 3, SL/auxin dependent (responsive to both TIS108 and PCIB); Cluster 4, auxin-dependent (PCIB-responsive, TIS108-unresponsive). Up arrows indicate induction, down arrows indicate reduction. Genes are indicated in italic. Abbr: DEGs, Differentially Expressed Genes; FPKM, fragments per kilobase of exon model per million mapped reads; LR, lateral roots; IAA, auxin; SL, strigolactones.

173x102mm (300 x 300 DPI)